Formation of crystalline nanosized titania in reverse micelles at room temperature

Dongbai Zhang, Limin Qi, Jiming Ma* and Humin Cheng

College of Chemistry and Molecular Engineering, Peking University, Beijing 100871, China

Shuttle-like crystalline TiO_2 nanoparticles were synthesized by hydrolysis of titanium tetrabutoxide in the presence of acids in NP-5 (Igepal CO-520)–cyclohexane reverse micelle at room temperature. Pure rutile nanoparticles were obtained at appropriate acid concentrations. The influences of various reaction conditions, such as concentration and type of acid, water content, H_2O/Ti molar ratio, and reaction time, on the formation, crystal phase, morphology, and size of the TiO_2 particles were investigated.

1 Introduction

Nanosized titanium dioxide particles have been the subject of a great deal of research because of their unique physicochemical properties and applications in the areas of pigments, catalysts and supports, fine ceramics, cosmetics, gas sensors, inorganic membranes, environmental purification, and dielectric materials.[1–9] The uses and performance for a given application are, however, strongly influenced by the crystalline structure, the morphology, and the size of the particles. As is well known, titanium dioxide exists mainly in three crystal forms, *i.e.* anatase, rutile, and brookite, each of which exhibits different physical properties and photochemical reactivity. Therefore, it is very important to develop methods for the synthesis of TiO_2 nanoparticles in which the particle size and the crystal structure of the products can be controlled.

Various methods have been used to produce titanium dioxide powders in the past two decades, such as the classic sulfate process, the chloride route, the sol–gel method,[10,11] the hydrothermal method,[12–14] and the gas condensation method.[15,16] To the best of our knowledge, all the crystalline TiO_2 particles reported are formed under harsh conditions, such as high temperatures with vigorous stirring,[12,14] or in the presence of mineralizers.[17] Recently, a reverse micelle method was successfully applied to synthesize TiO_2 nanoparticles[18–20] in reverse micelles or water/oil (W/O) microemulsion systems using titanium alkoxides as starting materials. The reverse micelle method has the unique advantage that the numerous nanoscale water pools existing in the micelle suspension are ideal microreactors for synthesizing nanoparticles. Up to now, the TiO_2 nanoparticles synthesized by using the reverse micelle method were all amorphous hydrates of TiO_2, hence the practical applications of this method were restricted.

In this paper, the preparation of pure rutile nanoparticles with widths of tens of nanometers and lengths of about 100 nm *via* a reverse micelle method at room temperature is presented. The synthesis is based on the hydrolysis of titanium tetrabutoxide under highly acidic conditions in a reverse micelle system, which leads to the formation of pure rutile nanoparticles or their aggregates at room temperature. The effects of the concentration and type of acid, the reaction time, and the water content in the reverse micelles on the morphology and crystalline structure of the obtained TiO_2 nanoparticle were investigated and possible mechanisms for the formation of the crystalline titania are briefly discussed.

2 Experimental procedure

2.1 Materials

The nonionic surfactant NP-5 (Igepal CO-520) was purchased from Aldrich and used without further treatment. Titanium tetrabutoxide, cyclohexane, and the acids were of A.R. grade, and the water used in this work was deionized and distilled.

2.2 Synthesis

A typical example of the synthesis of nanosize rutile titania is as follows. 73 µL of 2.5 M aqueous hydrochloric acid was added to 5 mL of 0.15 M NP-5–cyclohexane solution to form a reverse micelle system with a *w* value ($w = $ [H_2O]/[NP-5]) of 8. After complete mixing of the reverse micelle system, 135 µL of 1.25 M titanium tetrabutoxide–cyclohexane solution was added so that the parameter *h* ($h = $ [H_2O]/[Ti(OC$_4$H$_9$)$_4$]) was 28. Then, the mixture was allowed to stand at room temperature (about 22 °C) for 20 days. As mentioned above, different acids and various acid concentrations, and *w* and *h* values were employed to investigate how these factors influence the morphology, size, and crystalline structure of the TiO_2 particles.

2.3 Characterization

For the preparation of transmission electron microscopy (TEM) samples, the products were mixed with ethanol under sonication to form dispersions, and the dispersions were then repeatedly centrifuged at 3000 rpm and re-dispersed in clean ethanol under sonication to remove the unreacted titanium tetrabutoxide and unbound surfactant. A small amount of the final dispersion was dropped onto a Formvar-covered copper grid placed on filter paper. After evaporation of the solvent, conventional TEM micrographs were recorded on a JEOL JEM-200CX transmission electron microscope operating at 200 kV. Powder X-ray diffraction (XRD) patterns were recorded on a Rigaku Dmax-2000 diffractometer using Cu-Kα radiation.

3 Results and discussion

3.1 Influence of pH

The pH of the reaction medium has a significant effect on the crystal structure of the obtained TiO_2 nanoparticles. The TEM micrographs and electron diffraction patterns shown in Fig. 1
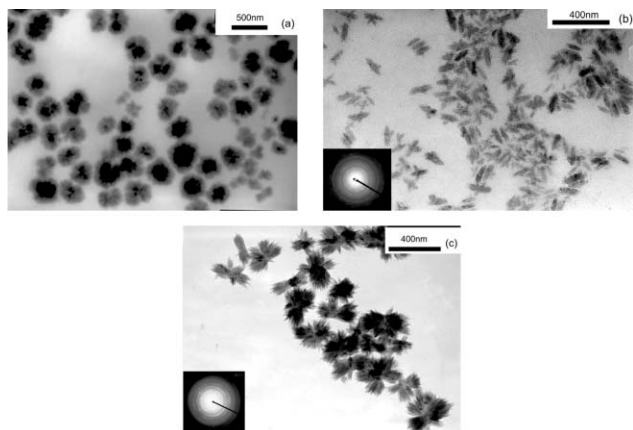
Fig. 1 TEM micrographs and electron diffraction patterns (insets) of TiO$_2$ particles formed at different hydrochloric acid concentrations: (a) 1.5 M; (b) 2 M; (c) 2.5 M.

provide direct information about the size, morphology, and crystalline structure of the TiO$_2$ particles obtained at different acidities. It can be seen from Fig. 1(a) that irregular and amorphous product was obtained when the concentration of hydrochloric acid in the aqueous phase of the reverse micelle system was below 2 M. When the acid concentration was increased to 2 M, the TiO$_2$ particles formed were found to be of a mixed crystal phase consisting of rutile and anatase [Fig. 1(b)]. The electron diffraction pattern suggests that the five fringe patterns observed, with spacings of 3.246, 2.088, 1.352, 2.447, and 1.653 Å correspond to rutile (110), (210), and (301) and anatase (103) and (211) spacings, respectively. Pure rutile phase was formed when the acid concentration was raised to 2.5 M [Fig. 1(c)]. In the electron diffraction pattern, the six fringe patterns, with spacings of 3.247, 2.491, 2.281, 1.686, 1.484, and 1.425 Å are consistent with rutile (110), (101), (200), (211), (002), and (310) spacings, and the corresponding XRD pattern is also shown in Fig. 2. When the acid concentration was further increased to 4 M, only amorphous TiO$_2$ particles were obtained.

In general, the titanium alkoxides hydrolyze rapidly in water and amorphous titanium dioxide hydrate is obtained. In order to obtain a crystalline product, hydrothermal treatment or calcination is usually necessary.[22] In the presence of acid, however, the hydrolysis of titanium alkoxides is inhibited to a certain degree, depending on the acidity of the aqueous phase. At high acidity, the hydrolysis of the titanium alkoxides may become very slow, which is favorable for the ordered arrangement of TiO$_2$ molecules and the crystalline phase
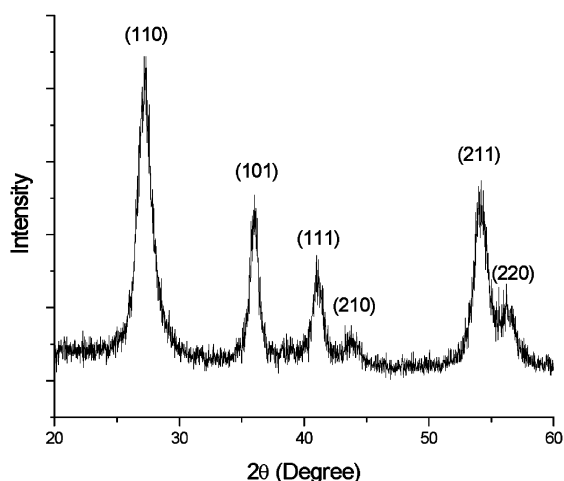
may be allowed to form, even at ambient temperature. Depending on the exact pH, both rutile and anatase can be formed through different condensation routes.[16] Anatase and rutile TiO$_2$ are constructed by linking TiO$_6$ octahedra in different bonding modes.[12] Anatase TiO$_2$ results from face-shared linking of TiO$_6$ octahedra and rutile TiO$_2$ is formed by edge-shared linking of TiO$_6$ octahedra along the *c*-axis. It has been reported that the concentration of TiCl$_4$, which is directly related to the acidity of the reaction medium, significantly influences the crystallization of rutile under hydrothermal conditions.[12] In the work of Wu and co-workers,[21,22] nanoparticles of rutile or anatase were prepared through microemulsion-mediated hydrothermal (MMH) and hydrothermal methods in the presence of hydrochloric or nitric acid. It was found that the concentration of the acid plays a dominant role in the hydrolysis and polycondensation of titanium(iv) n-butoxide, and higher HCl concentration favors rutile crystallization. Their product was a mixture of anatase and rutile when the concentration of hydrochloric acid was 1 M and pure rutile nanoparticles were obtained with HCl concentrations of 1.5 M or higher. Although the critical acid concentration for conversion from the mixture of rutile and anatase to pure rutile in the work of Wu and co-workers is some what different from our result, which probably is due to differences in the reaction temperature and reaction media, the general tendency to form pure rutile under higher acid concentrations is consistent. At even lower pH, the hydrolysis of the titanium alkoxides is essentially suppressed, and the amorphous product is obtained once again. In brief, our results indicate that crystalline TiO$_2$ nanoparticles can be obtained directly by hydrolysis of titanium tetrabutoxide in reverse micelle dispersions at an appropriate acidity; low or unduly high acidity causes the formation of amorphous products.

3.2 Influence of water content

To investigate the effect of the water content, *w*, ([H$_2$O]/[NP-5]) on the formation of TiO$_2$ particles, the hydrochloric acid concentration, *h* ([H$_2$O]/[Ti(OC$_4$H$_9$)$_4$]) and the reaction time were set at 2.5 M, 8, and 20 days, respectively, then the *w* value was adjusted from 3 to 12 (the largest value), and micrographs of the resulting products are shown in Fig. 2. It can be seen that when *w* = 3 [Fig. 3(a)], well-dispersed shuttle-like nanoparticles with widths of about 35–40 nm and lengths of about 150–160 nm are formed. Electron diffraction analysis indicated that the products had the crystalline structure of rutile. On increasing the *w* value from 3 to 5, both the width and the length of the TiO$_2$ nanoparticles increased slightly, but the shuttle-like morphology of the particles was unchanged. When *w* = 10 [Fig. 3(b)], a lot of petal-like particles formed, which are apparently aggregates of the shuttle-like particles and show the same crystalline structure. In our work, the water pools of the reverse micelles act as microreactors for the hydrolysis of the titanium tetrabutoxide. Thus, as the water content increases, the water pools become larger and so are liable to inosculate with each other, hence rutile nanoparticles from different pools will form aggregates, leading to the variation in morphology from shuttle-like to petal-like with increasing *w* values. In the case of *w* = 12, however, the

Fig. 2 XRD pattern of TiO$_2$ particles obtained with a hydrochloric acid concentration of 2.5 M. The indexed peaks are due to rutile.
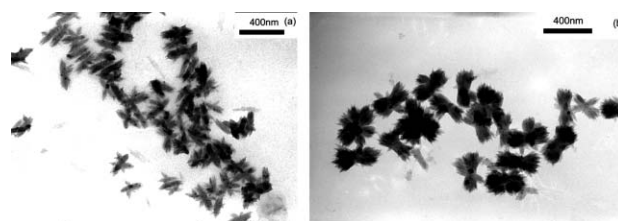
Fig. 3 TEM micrographs of TiO$_2$ particles formed at different water contents: (a) *w* = 3; (b) *w* = 10.
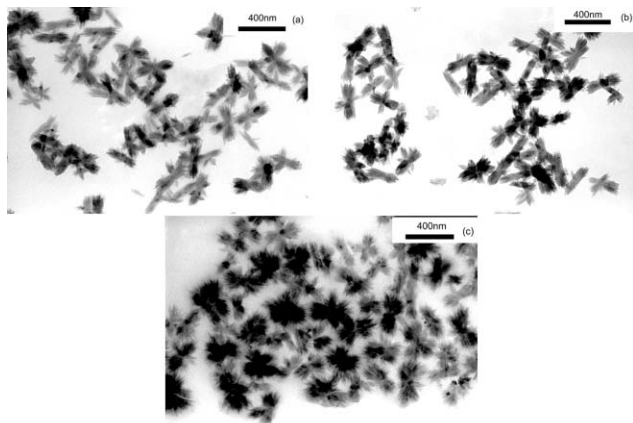
Fig. 4 TEM micrographs of TiO₂ particles formed at different water to Ti(OC₄H₉)₄ molar ratios: (a) $h = 10$; (b) $h = 20$; (c) $h = 36$.

Fig. 5 TEM micrographs of TiO₂ particles formed in the presence of different acids: (a) nitric acid; (b) sulfuric acid; (c) phosphoric acid.

obtained TiO₂ particles showed the same petal-like morphology, but a mixed crystalline phase consisting of rutile and anatase, probably due to disruption of the reverse micelles during the reaction with such a high water content.

3.3 Influence of H₂O/Ti ratio

The TEM micrographs in Fig. 4 show the effect of the h value, the water to titanium tetrabutoxide molar ratio, on the TiO₂ nanoparticles formed in reverse micelles at constant w value of 8, an acid concentration of 2.5 M, and a reaction time of 20 days. When h is less than 6, which is lower than the coordination number of the Ti(IV) ions, the amount of the water in the water pools of the reverse micelle system is not sufficient to completely hydrolyze the Ti(OC₄H₉)₄ and, hence, the process of crystallization is hindered, so only spherical amorphous TiO₂ particles can be obtained. On increasing h to greater than 10, the products changed from amorphous to crystalline rutile. Fig. 4 shows the morphology and electron diffraction patterns of TiO₂ particles formed at h values of 10, 20, and 36, respectively. It is obvious that the size of the primary particles is barely influenced by the h value, but the shuttle-like particles aggregate into petal-like particles with increasing h, and form flower-like aggloromates when $h = 36$. A possible reason for this may be that increasing h values are usually accompanied by an acceleration of the Ti(OC₄H₉)₄ hydrolysis process, and the crystalline TiO₂ particles formed are liable to aggregation in or between the water pools of the reverse micelle dispersion.

3.4 Influence of the nature of the acid

Four different acids, hydrochloric acid, nitric acid, sulfuric acid, and phosphoric acid, were used to adjust the pH of the aqueous phase in order to examine the effect of the nature of the acid on the morphology, crystalline phase, and particle size of the TiO₂ nanoparticles formed. The values of w and h were set to 8 and 28, respectively, the acid concentrations were all controlled to be equivalent to 2.5 M hydrochloric acid, and the other conditions were kept the same as those mentioned in synthesis procedure. The results demonstrate that the nature of the acid has marked effects on the crystalline phase, morphology, and particle size of the TiO₂ nanoparticles. From Fig. 5, it can be seen that when replacing hydrochloric acid with nitric acid, the obtained TiO₂ particles retain the shuttle-like morphology and rutile phase [Fig. 5(a)], but the particle sizes are slightly smaller than those obtained using hydrochloric acid, showing widths of 20–25 nm and lengths of about 120 nm. On the other hand, using sulfuric or phosphoric acid to adjust the pH of the aqueous phase meant that crystalline TiO₂ particles were not formed at all the acid
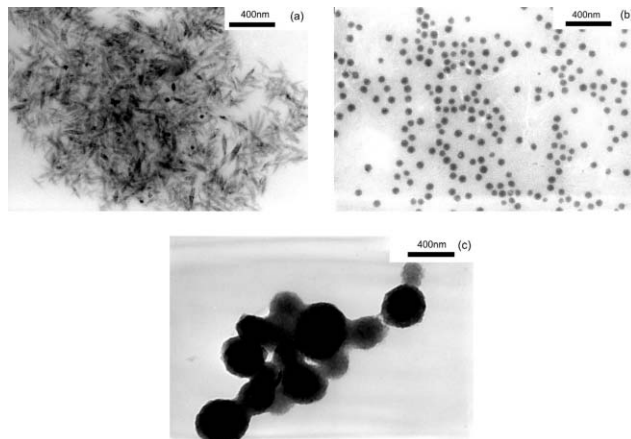
concentrations used in the experiment. Instead, amorphous spherical TiO₂ particles were obtained; the particles obtained by using sulfuric acid were uniform small spheres with diameters of about 40 nm [Fig. 5(b)], in contrast to the large spheres with diameters of about 240 nm that resulted from using phosphoric acid [Fig. 5(c)].

The formation of the crystalline TiO₂ particles depends on the rearrangement of the TiO₂ molecules in an ordered manner. It has been well documented that NO₃⁻ and Cl⁻ anions show a weaker affinity for titanium ions in aqueous solution than do CH₃COO⁻ and SO₄²⁻ anions.[22–24] The strong affinity of SO₄²⁻ for titanium inhibits the structural rearrangement of the TiO₂ molecules and, subsequently, the phase transformation. In the synthesis of TiO₂ using a microemulsion as the reaction medium, H₂SO₄ may accordingly inhibit the generation of crystalline phases of TiO₂, due to the suppression of molecular rearrangement, and the product thus remains amorphous. This may also be the case with H₃PO₄, which is probably why only amorphous TiO₂ spheres were obtained in the presence of sulfuric and phosphoric acid.

3.5 Influence of reaction time

Fig. 6 shows TEM micrographs of TiO₂ particles obtained under standard conditions with different reaction times. It is obvious that prolonging the reaction time will make the particles grow and agglomerate. After a reaction time of 5 days [Fig. 6(a)], well-dispersed shuttle-like particles with widths of 30 nm and lengths of 120 nm were formed. As the reaction time was increased to 10 days, the shuttle-like particles began to aggregate and form petal-like bundles of particles [Fig. 6(a)].
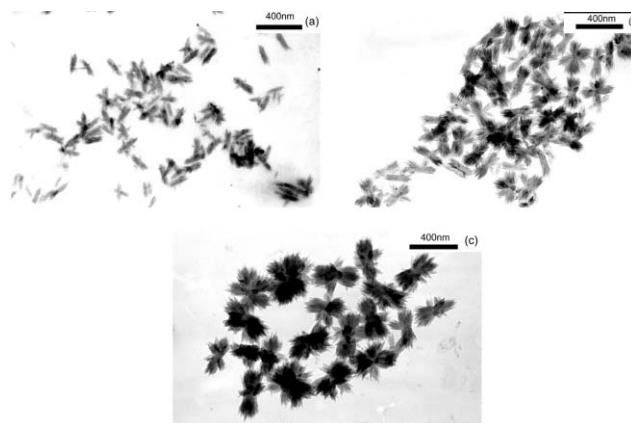
Fig. 6 TEM micrographs of TiO₂ particles formed after different reaction times: (a) 5 days; (b) 10 days; (c) 20 days.

After 20 days reaction, the particle bundles begin to aggregate and, eventually, flower-like particles are obtained [Fig. 6(c)].

3.6 Mechanism of formation of rutile nanoparticles

Titanium(IV) alkoxides are, in general, very reactive due to the presence of highly electronegative OR groups that stabilize the titanium cation in its highest oxidation state and render Ti(IV) very susceptible to nucleophilic attack. According to the concepts of the partial charge model,[14] the first step of hydrolysis of titanium cations leads to the formation of $[Ti(OH)(OH_2)_5]^{3+}$ species which are stable under strongly acidic conditions and are not able to condense with each other because of the strong mutual repulsion between the complex ions as a result of the positive charge of the hydroxo complex. Condensation to both rutile and anatase starts when the solution acidity is high enough to allow further deprotonation and intramolecular oxolation to $[TiO(OH)(OH_2)_4]^+$, which can undergo intramolecular deoxolation to $[Ti(OH)_3(OH_2)_3]^+$, depending on the exact pH. In the lower pH region, deoxolation does not occur and oxolation leads to linear growth along the equatorial plane of the cations. This process, followed by oxolation between the resulting linear chains, leads to rutile formation. At higher pH values, when deoxolation takes place, condensation can proceed along apical directions, leading to the skewed chains of the anatase structure. Our results indicate that the mixed crystal phase formed at relatively higher pH (2 M hydrochloric acid) was converted into pure rutile at lower pH (2.5 M hydrochloric acid), which is consistent with the above-mentioned mechanism. In more acidic regions, condensation and crystallization may be unable to occur at ambient temperature due to the strong mutual repulsion between the complex ions formed under the conditions mentioned above, leading to the formation of amorphous TiO_2.

4 Conclusion

Nanosize titanium dioxide particles with pure rutile crystalline structures were obtained *via* a reverse micelle method under strongly acidic conditions at room temperature. The reaction conditions have significant effects on the crystal structure, morphology, and particle size of the products. The acidity, the type of acid used, and the microenvironment of the reverse micelles are the key factors affecting the formation of rutile at room temperature. Prolonged reaction times and increasing the $[H_2O]/[NP-5]$ and $[H_2O]/[Ti(OC_4H_9)_4]$ ratios leads to agglomeration of the particles.

References

1 T. Moritz, J. Reiss, K. Diesner, D. Su and A. Chemseddine, *J. Phys. Chem. B*, 1997, **101**, 8052.
2 J. Karch, R. Birriger and H. Gleiter, *Nature*, 1987, **330**, 556.
3 M. R. Hoffmann, S. T. Martin, W. Choi and D. W. Bahnemann, *Chem. Rev.*, 1995, **95**, 69.
4 A. Fujishima and K. Honda, *Nature*, 1972, **238**, 37.
5 M. A. Fox and M. T. Dulay, *Chem. Rev.*, 1993, **93**, 341.
6 R. J. Gonzalez, R. Zallen and H. Berger, *Phys. Rev. B*, 1997, **55**, 7014.
7 K.-N. P. Kumar, K. Keizer and A. J. Burggraaf, *J. Mater. Chem.*, 1993, **3**, 1141.
8 R. Wang, K. Hashimoto and A. Fujishima, *Nature*, 1997, **388**, 431.
9 P. A. Mandelbaum, A. E. Regazzoni, M. A. Blesa and S. A. Bilmes, *J. Phys. Chem. B*, 1999, **103**, 5505.
10 M. Schneider and A. Baiker, *J. Mater. Chem.*, 1992, **2**, 587.
11 B. E. Yoldas, *J. Mater. Sci.*, 1986, **21**, 1087.
12 H. Cheng, J. Ma, Z. Zhao and L. Qi, *Chem. Mater.*, 1995, **7**, 663.
13 C. C. Wang and J. Y. Ying, *Chem. Mater.*, 1999, **11**, 3113.
14 S. T. Aruna, S. Tirosh and A. Zaban, *J. Mater. Chem.*, 2000, **10**, 2388.
15 L. Shi, C. Li, A. P. Chen, Y. H. Zhu and D. Y. Fang, *Mater. Chem. Phys.*, 2000, **66**, 51.
16 J. Rubio, J. L. Oteo, M. Villegas and P. Duran, *J. Mater. Sci.*, 1997, **32**, 643.
17 K.-N. P. Kumar and K. Keizer, *J. Mater. Chem.*, 1993, **3**, 923.
18 F. Cot, A. Larbot, G. Nabias and L. Cot, *Nanostruct. Mater.*, 1998, **10**, 2175.
19 T. Hirai, H. Sato and I. Komasawa, *Ind. Eng. Chem. Res.*, 1993, **32**, 3014.
20 G. L. Li and G. H. Wang, *Nanostruct. Mater.*, 1999, **11**, 663.
21 M. M. Wu, G. Lin, D. H. Chen, G. G. Wang, D. He, S. H. Feng and R. R. Xu, *Chem. Mater.*, 2002, **14**, 1974.
22 M. M. Wu, J. B. Long, A. H. Huang, Y. J. Luo, S. H. Feng and R. R. Xu, *Langmuir*, 1999, **15**, 8822.
23 C. Sanchez, J. Livage, M. Henry and F. Babonneau, *J. Non-Cryst. Solids*, 1988, **100**, 65.
24 E. Matijevic, *J. Colloid Interface Sci.*, 1977, **58**, 374.